

Vortex motion in two-dimensional arrays of small, underdamped Josephson junctions

T. S. Tighe, A. T. Johnson, and M. Tinkham

Physics Department and Division of Applied Sciences, Harvard University, Cambridge, Massachusetts 02138

(Received 21 May 1991)

We report measurements on vortex motion in two-dimensional arrays of small, underdamped, superconducting tunnel junctions, having charging energies on the order of the Josephson coupling energy. Our measurements are consistent with a simple model of the array as a periodic pinning potential, with measured values of the depinning current and the barrier energy in general agreement with the predicted values. Although the individual junctions are underdamped, the vortices move in an overdamped manner, with a critical velocity. We report preliminary evidence for macroscopic quantum tunneling of vortices.

Vortex motion in superconductors has been the subject of much theoretical and experimental work.¹ Two-dimensional (2D) arrays of Josephson junctions provide an excellent system for studying this motion, as the pinning potential is theoretically known.^{2,3} Most of the existing work concentrates on arrays with classical, overdamped junctions, where the charging energy E_c ($=e^2/2C$, C the junction capacitance) is negligible and the McCumber parameter β_c is less than 1.²⁻⁴ Modern lithographic techniques allow one to fabricate arrays of small S - I - S tunnel junctions which are underdamped ($\beta_c > 1$) and have an appreciable charging energy.⁵ This research studies the motion of vortices in arrays of underdamped junctions and examines the effect of nonzero charging energies.

Each unit cell of a Josephson junction array is a pinning site. Between adjacent sites there is an energy barrier E_b , which is proportional to the Josephson coupling energy E_j . A pinned vortex can overcome the barrier by thermal activation or by quantum mechanical tunneling. In the presence of a bias current, a vortex can also be forced over the barrier by a $\mathbf{j} \times \mathbf{B}$ force, its motion being perpendicular to the current direction. In arrays of overdamped junctions, the vortices move viscously and tunneling is negligible. With our arrays of underdamped junctions, however, one might expect that the vortices move with little damping, and that tunneling may be measurable. We do see preliminary evidence of this tunneling of vortices. Our measurements indicate, however, that despite the low damping environment vortices move in an overdamped manner.

We have fabricated and measured two-dimensional arrays of Sn-SnO_x-Sn tunnel junctions. The data presented here will focus on two arrays, each 50 columns by 70 rows, with individual junction area of 0.1 μm^2 . The current direction is along the columns, so that the minimum number of junctions through which the current must travel is 70. The arrays are made using electron-beam lithography with a shadow evaporation technique.⁶ The average normal resistances of the individual junctions for samples A and B are, respectively, 24 and 201 k Ω . The geometric capacitance of the individual junctions

for both arrays is roughly 2.5 fF, which corresponds to a charging energy of $E_c/k_B = 350$ mK. E_j is approximated by $E_j = (h/8e^2)(\Delta/R_n)$,⁷ where Δ is the superconducting energy gap ($2\Delta \approx 1.2$ meV for Sn), and R_n is the normal-state resistance. E_j/k_B for samples A and B are, respectively, 910 and 110 mK. In A, E_j is larger than E_c , while in B this is reversed.

We measure the arrays in a dilution refrigerator at temperatures down to 50 mK. To determine whether self-heating prevents the sample from reaching these low nominal temperatures, we measured the differential resistance of sample B in a magnetic field of about 50 G. At this field,⁸ the resistance varies strongly over the entire nominal temperature range of our measurements, a good indication that sample heating is not a serious limitation in reaching low temperatures. This test is limited to the region where the current-voltage (I - V) curves are continuous, roughly at powers below 100 fW, so we cannot rule out self-heating at the larger powers used in the measurements of Figs. 1 and 2. In Fig. 3, however, the measurements of the low-voltage resistance R_0 are all made at powers below 100 fW, so that we believe the measured temperature accurately reflects the sample temperature.

We measure I - V characteristics by a standard four-probe technique. The leads coming from the sample are attached to the measuring circuit through 5 k Ω resistors, nominally at the sample temperature. These resistors allow the sample to see cold Johnson noise and protect the sample from any voltage spikes that occur. To minimize external noise, we use a battery-powered current source, analog amplifiers, and an X - Y chart recorder. All measurements are made inside an electrically shielded room. Cold microwave filters⁹ had not been installed for the measurements on sample A. They were used with sample B, however, and with another sample with a normal resistance nearly equal to that of A. The measurements on this third sample are very similar to those on A, allowing us to use the much more extensive data for A with confidence.

Vortices are introduced by applying an external magnetic field. The field strength is described by f , the number of flux quanta, $\Phi_0 = hc/2e$, per unit cell. We deter-

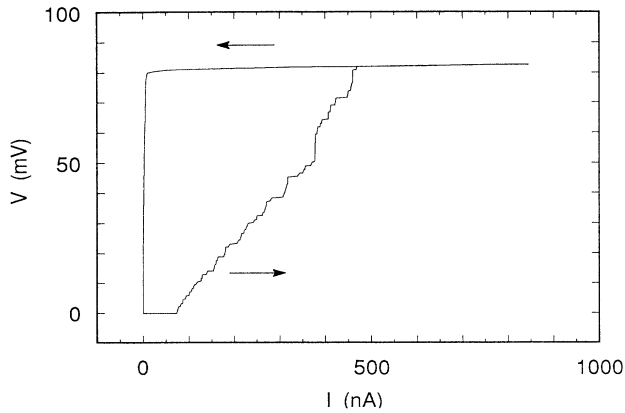


FIG. 1. Current-voltage (I - V) characteristics for sample A at 90 mK. The array is 50 by 70 unit cells, with average individual junction normal resistance of 24 k Ω . The curve is hysteretic, with the arrows indicating the direction of the sweeping current. At this current and voltage scale, the shape of the curve is largely independent of frustration.

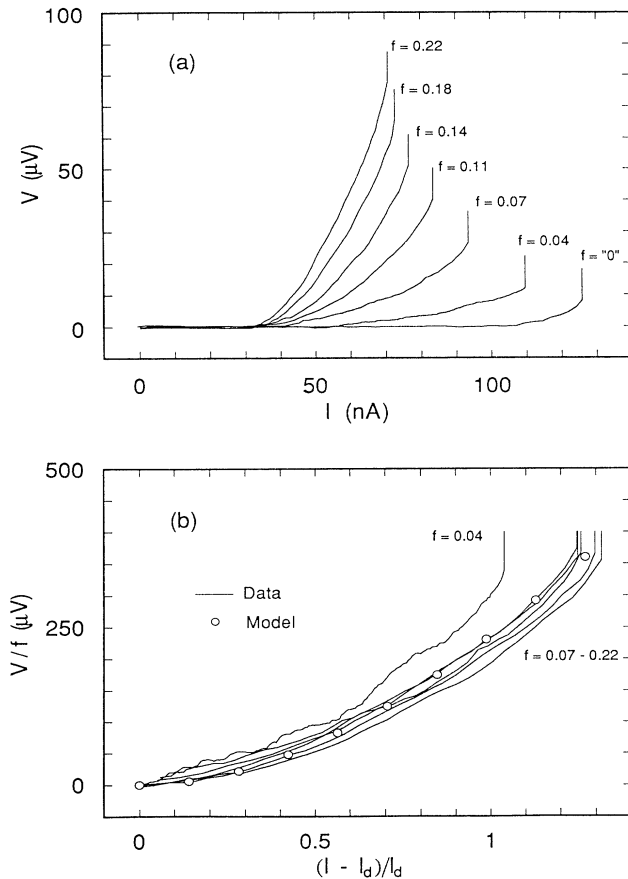


FIG. 2. I - V characteristics for sample A at 50 mK, before the first step. The vertical scale has been expanded by roughly a factor of 1000 over Fig. 1. The different curves are for different values of frustration, f . In (a), f is increased uniformly from roughly 0 to 0.22. In (b), these curves have been replotted with different axes, showing a rough collapse into a common trend, along with a curve (hollow circles) modeling the data, as described in the text.

mine f to within ± 0.01 by measuring the field dependence of the I - V characteristics and interpolating between the integer values, which are readily identified by sharp voltage minima. We do see evidence, discussed below, for an energy barrier to introducing field-induced vortices. As discussed by van der Zant,¹⁰ this effect is due to the finite sample size, and dominates at very low frustrations (at or below $f=0.0009$ for a sample with similar dimensions to ours). The measurements presented here are made at high enough frustrations ($f > 0.01$) such that this effect does not dominate, and vortices are not prevented from entering the sample. For sample A, thermally generated free vortices can be neglected because the data presented here are made below the Kosterlitz-Thouless transition temperature, T_{KT} .^{4,10,11} The measurements to which we attribute vortex quantum tunneling in sample B are made at a temperature also below its T_{KT} .

Figure 1 shows an I - V curve for sample A at a temperature of 90 mK. The curve is hysteretic: increasing the current from zero, no voltage (on this scale) appears across the array until the critical current of the first step, I_c , is reached. The voltage then jumps in many steps to roughly 70 times the gap voltage. These steps result from individual or multiple rows switching from a zero voltage state to a gap voltage state, as has been previously reported.¹² Upon decreasing the current from this state, the voltage does not drop down immediately, but remains high until very near zero current (on the order of 10 pA). Then, finally, the voltage drops back down to zero. This drop occurs in discrete jumps, but only the last few are discernible, and then only on an expanded current scale. Sample B shows similar behavior.

The distribution of currents where jumps occur is most likely due to variation in junction parameters. Tests on a

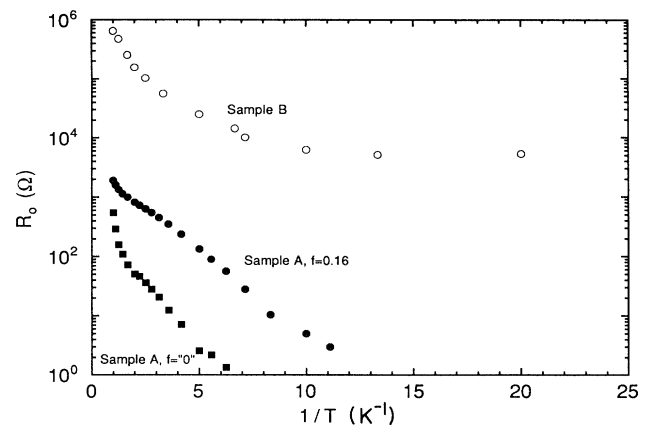


FIG. 3. Low-current ($I < I_d$) resistance R_0 vs inverse temperature for sample A (filled symbols) and sample B (hollow symbols). For A, two curves are shown for different frustrations, $f \approx 0$ and $f=0.16$. For B, the frustration was not determined. Neither curve for A, the lower resistance array, shows any sign of leveling out at low temperatures. The higher resistance array, B, does show a leveling out, however, which is evidence for quantum tunneling of vortices.

one-dimensional array of ten junctions, fabricated in the same way, show a variation of critical currents of about 40%, and a standard deviation of 15% about the mean. This fairly wide distribution possibly explains the spread of steps in the 2D array.

Using higher voltage sensitivity to study the region before the first step, where all the rows are nominally in the zero-voltage state, we see a small voltage. This voltage is evidence for vortex motion, as the measured voltage is proportional to the average vortex velocity. Figure 2(a) shows these features, with the vertical scale of Fig. 1 expanded by a factor of 1000. The I - V curves are dependent on the frustration f : the sample develops little voltage for $f \approx 0$, where few vortices are present, but the voltage develops much more rapidly for higher f , where there are more vortices.

For all the values of frustration, no voltage develops until a certain value of current is exceeded, the depinning current, I_d . This depinning current is a measure of the pinning barrier, E_b : the vortices are pinned until forced over the barrier by a sufficiently strong bias current [in the absence of thermal activation, which we believe is negligible at 50 mK (Ref. 13)]. For currents stronger than I_d , the system is in a flux flow regime, with damping largely determining the vortex motion. I_d for an isolated vortex was calculated numerically by Lobb, Abraham, and Tinkham³ (LAT) to be $I_d = 0.1NI_{c0}$, where I_{c0} is the unfluctuated critical current of a single junction and N is the number of columns. We estimate I_{c0} by using the result $I_{c0}R_n = \pi\Delta/2e$ ($\approx 9.1 \times 10^{-4}$ V for Sn). For sample A, this yields $0.1NI_{c0} = 190$ nA. This value is most likely an overestimate as it is derived for an array of identical junctions, while samples A and B have a spread in junction parameters. (The R_n we give is the measured value, an average over all the junctions.) Vortices will depin in the weakest row first, at a current below the average depinning current. To a first approximation, we can correct for this by multiplying the I_{c0} estimated for a uniform array by the ratio of the measured I_c of the first row to that of the average measured I_c . From Fig. 1 this ratio is 0.24, which gives $0.1NI'_{c0} = 46$ nA, with I'_{c0} being the corrected value.

At low values of frustration, the depinning current we measure is somewhat dependent on f , which makes it difficult to compare with that calculated by LAT. This dependence is thought to be due to an energy barrier to the introduction of field-induced vortices.¹⁴ For higher fields, where this effect is smaller and where the depinning current becomes independent of frustration, we measure $I_d \approx 32$ nA. Within the approximate method we use to take account of inhomogeneities, this is in reasonable agreement with the estimated value of $0.1NI'_{c0} = 46$ nA.

In Fig. 2(a), f is increased from $f \approx 0$ to $f = 0.22$ in steps of roughly 0.035. We see a regular increase with f in the developed voltage. If the independent vortex approximation held true for all frustrations, the curves in Fig. 2(a) should scale with f . To a large extent they do, except that the depinning current is dependent on f . In Fig. 2(b), we take this into account in a simple way by plotting V/f vs $(I - I_d)/I_d$. This is a reasonable choice

as in the “flux flow” regime, the voltage due to vortex velocity is proportional to the number of vortices multiplied by $(I - I_d)R_n$, with R_n inversely proportional to I_{c0} and hence I_d . All the curves collapse into a common trend, except the curve at the smallest frustration, where the uncertainties in f and I_d are the largest.

By taking explicit account of junction inhomogeneities, we can improve our earlier simple approximation. Treating the rows as separate, the measured voltage is the sum of voltages from each row, each being linear in $(I - I_{dm})$, where I_{dm} is the depinning current for the m th row. Taking the distribution of critical currents of the rows from Fig. 1, one can compute this sum. However, as it appears this distribution is approximately uniform, we can analytically determine this sum in a continuum limit. The resulting curve is given by the hollow circles in Fig. 2(b) with one free parameter, the vortex viscosity. Though only a crude approximation, this model indicates that the upward curvature of the data curves has a simple explanation.

As all the individual junctions are underdamped, we might expect the vortex motion to be underdamped. This can be seen by an argument of Rzchowski *et al.*² which makes a direct analogy between the motion of a vortex and the dynamics of an individual junction. He showed that the equation of motion for a single vortex in an array is theoretically given by

$$\frac{d^2}{dt^2} \left[\frac{2\pi x}{a} \right] + \frac{1}{R_n C} \frac{d}{dt} \left[\frac{2\pi x}{a} \right] + \frac{8k}{\hbar^2} E_c E_j \sin \left[\frac{2\pi x}{a} \right] - \frac{8E_c}{\hbar e} I = 0, \quad (1)$$

where x is the vortex position along a line passing through cell centers, a is the lattice spacing along a column, I is the bias current, and k is defined by $E_b = kE_j$. A similar equation describing the phase dynamics of a *single* junction is

$$\frac{d^2\theta}{dt^2} + \frac{1}{R_n C} \frac{d\theta}{dt} + \frac{8}{\hbar^2} E_c E_j \sin\theta - \frac{4E_c}{\hbar e} I = 0. \quad (2)$$

Equating $2\pi x/a$ with θ , these two equations are identical, apart from numerical prefactors of order 1. Effects of the leads, which change the damping term in Eq. (2) for measurements on individual junctions,¹⁵ are thought not to be important for junctions in an array, as they are shielded from the environment by the other junctions.

In this analogy to the “washboard” model of single junctions, which Eq. (2) describes, we might expect that once the vortex initially escaped its well, it would continue to run freely. In this case we would see a hysteretic voltage jump at the depinning current, similar to the hysteretic jump at the critical current for a single junction. However, we do not see a jump in voltage or any hysteresis at I_d , and the motion appears to be overdamped. The vortex motion in sample B also appears overdamped. Numerical simulations^{16,17} of arrays of underdamped Josephson junctions found that the junctions near a moving vortex are caused to oscillate. Thus a moving vortex

loses energy to its “wake,” which possibly provides the damping mechanism which keeps vortices from running freely after initially being depinned.

The numerical work of Nakajima and Sawada¹⁶ (NS) also showed a maximum vortex velocity. When the frequency of phase slips due to a moving vortex reaches roughly half the plasma frequency of the individual junction, the simple description of vortex motion fails (a succession of vortex-antivortex pairs is created behind the initial vortex). In our measurements this corresponds to a row switching from the zero-voltage state to the gap voltage state. In Fig. 2(b) we observe evidence for such a critical velocity, namely, a constant value of V/f where the first row switches. (As the measured voltage per vortex is proportional to vortex velocity, this maximum voltage per vortex suggests a critical vortex velocity.) Using the maximum value of V/f from Fig. 2(b), $360 \mu\text{V}$, this corresponds to a frequency of phase slips equaling 1.5×10^{10} rad/s. As this value is computed for an array with homogeneous junctions, it likely underestimates the actual value for the frequency in the active rows. The same approximation used to model the curves of Fig. 2(b) gives 2.0×10^{11} rad/s for vortices in the fastest moving rows. Within our simple approximations, this roughly agrees with the estimated value of NS of $0.5\omega_p = 1.0 \times 10^{11}$ rad/s.

So far we have concentrated on vortex motion for currents larger than the depinning current. However, for currents less than I_d , a vortex can still move from well to well via two mechanisms. It can hop over the barrier by thermal activation, and it can tunnel through it quantum mechanically. At high temperatures, thermal activation dominates. Making our direct analogy to the washboard model for a single junction, the measured voltage will just be proportional to the rate of hopping along the direction of force (preferred) minus the rate of hopping against the direction of force (not preferred). Experimentally we find that this voltage is proportional to the bias current, allowing us to define a resistance R_0 . For temperatures where thermal activation dominates, this resistance is predicted to be^{18,19}

$$R_0 \propto \frac{h}{4e^2} \frac{\hbar\omega_0}{k_B T} \exp\left[\frac{-E_b}{k_B T}\right], \quad (3)$$

where $\omega_0 = (1/\hbar)(8E_c E_b)^{1/2}$ is the classical frequency of oscillations of the vortex in the bottom of the well. While initially used to describe single junctions, this R_0 should apply to vortex motion as well under the direct analogy between the two. Including a factor of frustration times the number of active rows turns Eq. (3) into an approximate equality. This does not take into account vortices jumping multiple wells, which was shown to be important in the prefactor of Eq. (3) by Martinis and Kautz.²⁰ However, because we are mostly interested in the energy barrier E_b , given approximately by the slope of $\ln(R_0 T)$ vs $1/T$, we will not take multiple jumps into account.

The vortex also can tunnel through the barrier quantum mechanically. The charging energy E_c , plays an important role in tunneling. Increasing E_c over E_b increases the probability for tunneling. This is true until

$E_c \gg E_b$ when the vortices become completely delocalized and the vortex description of the system is inappropriate. The maximum value of E_c/E_j where the vortex description still has meaning has been estimated to be about 5.²¹ Thus, both samples A and B, with $E_c/E_j = 0.3$ and 3, respectively, fall within this limit.

Quantum tunneling is expected to dominate at low temperatures, when thermal activation becomes negligible. R_0 , a measure of vortex motion, will have then two regions: at higher temperatures thermal activation dominates and R_0 will decrease exponentially with temperature. Below some crossover temperature T_{cr} , quantum tunneling will dominate and R_0 will become temperature independent. In analogy to the single-junction problem, T_{cr} is roughly given by $k_B T_{cr} \approx \hbar\omega_0/2\pi$.²²

The measurements shown in Fig. 2 for sample A were made at $T = 50$ mK, where R_0 is zero to within our measuring limits. At higher temperatures, the I - V curves look very much as in Fig. 2, with the exception that R_0 is measurable, and can even become large.

Figure 3 shows R_0 vs temperature for samples A and B. For Sample A, two different sets of data are shown, for $f \approx 0$ and $f = 0.16$. The general trend is for R_0 to increase as the temperature increases, which reflects the increasing thermal activation of vortices. The values for R_0 at $f \approx 0$ are much less than those for $f = 0.16$ simply because of the far smaller number of vortices present. We cannot measure R_0 for the lower temperatures because it falls below our noise level, about 1 Ω .

From the slope of these curves, we determine the energy barrier for the $f = 0.16$ case for sample A. We measure $E_b = 1.0E_j$, higher than that predicted by LAT, $E_b = 0.2E_j$. The barrier is stronger than expected by a factor of 5, but in line with measurements by other groups which have found barriers anywhere from $0.34E_j$ to $2E_j$.^{2,23} Taking into account sample inhomogeneity, which suggests that vortices first move in the rows with weaker barriers, $1.0E_j$ possibly is a measure of these weaker barriers, so that the average barrier height is larger, being further away from the estimated value. LAT does neglect extrinsic pinning by local inhomogeneities and charging effects, however, both of which may be important. For sample B, it is not possible to determine E_b in this way, as there is no real linear region in $\ln(R_0 T)$ vs $1/T$.

In sample A, we do not see evidence of quantum tunneling. There is no region at low temperatures where R_0 levels off. The estimated crossover temperature for A is within the range $T_{cr} \approx 100$ – 250 mK, so it is reasonable that the leveling off occurs below our noise level. In sample B, however, the ratio of charging energy to Josephson energy is larger than that for sample A, and we might expect to see a larger amount of tunneling, with a measurable value of R_0 as T approaches zero. This is the case, as seen in Fig. 3. R_0 for sample B becomes temperature independent for $T < 100$ mK, evidence for the quantum tunneling of vortices. Here, the estimated value of T_{cr} is within the range 40 – 100 mK. In Fig. 3 the temperature at which R_0 begins to level off is roughly 100 mK, consistent with the estimated value. This evidence, however,

is preliminary, as the value of the frustration was not determined before an unknown event degraded sample B.

In conclusion, we have studied vortex motion in 2D arrays of underdamped Josephson junctions. The vortices are pinned in potential wells for small bias currents, but at a depinning current I_d , they overcome the barrier between the wells and start flowing. Despite the junctions in the array being underdamped, vortices move in an overdamped manner. One possible explanation is that vortices lose energy to junctions in their "wake," by causing them to oscillate at the plasma frequency. We measure a maximum vortex velocity, beyond which rows in the array start switching to the gap voltage state. No vortex tunneling was observed for the lower resistance array, but preliminary evidence for tunneling was found in

the higher resistance array. These higher resistance arrays will be the focus of further research, searching for more conclusive evidence on quantum tunneling of vortices.

Near completion of this manuscript, we learned of recent work which reports similar results.²⁴

We gratefully acknowledge the assistance of D. B. Ephron in developing the techniques for making small-junction arrays in this research group. This research was supported in part by the National Science Foundation Grant No. DMR-89-12927, the U.S. Office of Naval Research Grant No. N00014-89-J-1565, and the Joint Services Electronic Program Grant No. N00014-89-J-1023.

-
- ¹R. P. Huebener, *Magnetic Flux Structures in Superconductors*, (Springer-Verlag, Berlin, New York, 1979); A. M. Campbell and J. E. Evetts, *Adv. Phys.* **21**, 199 (1972).
- ²M. S. Rzchowski, S. P. Benz, M. Tinkham, and C. J. Lobb, *Phys. Rev. B* **42**, 2041 (1990).
- ³C. J. Lobb, David W. Abraham, and M. Tinkham, *Phys. Rev. B* **27**, 150 (1983).
- ⁴D. J. Resnick, J. C. Garland, J. T. Boyd, S. Shoemaker, and R. S. Newrock, *Phys. Rev. Lett.* **47**, 1542 (1981); David W. Abraham, C. J. Lobb, M. Tinkham, and T. M. Klapwijk, *Phys. Rev. B* **26**, 5268 (1982); R. F. Voss and R. A. Webb, *ibid.* **25**, 3446 (1982); J. P. Carini, *ibid.* **38**, 63 (1988).
- ⁵L. J. Geerligs, M. Peters, L. E. M. de Groot, A. Verbruggen, and J. E. Mooij, *Phys. Rev. Lett.* **63**, 326 (1989).
- ⁶G. J. Dolan, *Appl. Phys. Lett.* **31**, 337 (1977).
- ⁷V. Ambegaokar and A. Baratoff, *Phys. Rev. Lett.* **10**, 486 (1963).
- ⁸The field is needed because in much smaller fields, the resistance does become temperature independent below roughly 100 mK. As discussed below, we attribute this to quantum mechanical vortex tunneling. By decreasing the energy barrier with a sufficiently strong field, we can increase the thermal activation of the vortices enough so that it dominates over tunneling for our entire temperature range.
- ⁹J. Martinis, M. Devoret, and J. Clarke, *Phys. Rev. B* **35**, 4682 (1987).
- ¹⁰H. S. J. van der Zant, H. A. Rijken, and J. E. Mooij, *J. Low Temp. Phys.* **79**, 289 (1990).
- ¹¹J. M. Kosterlitz and D. J. Thouless, *J. Phys. C* **6**, 1181 (1973).
- ¹²H. S. J. van der Zant, C. J. Muller, L. J. Geerligs, C. J. P. M. Harmans, and J. E. Mooij, *Phys. Rev. B* **38**, 5154 (1988).
- ¹³Using 100 fW as a power level for which we believe self-heating does not heat the sample appreciably above its nominal measured temperature, a typical depinning current of 50 nA corresponds to 2 μ V, which is within our resolution to measure the depinning current.
- ¹⁴J. E. Mooij (private communication).
- ¹⁵A. T. Johnson, C. J. Lobb, and M. Tinkham, *Phys. Rev. Lett.* **65**, 1263 (1990).
- ¹⁶K. Nakajima and Y. Sawada, *J. Appl. Phys.* **52**, 5732 (1981).
- ¹⁷P. Bobbert (private communication).
- ¹⁸Y. M. Ivanchenko and L. A. Zil'berman, *Zh. Eksp. Teor. Fiz.* **55**, 2395 (1968) [*Sov. Phys. JETP* **28**, 1272 (1969)].
- ¹⁹M. Iansiti, A. T. Johnson, C. J. Lobb, and M. Tinkham, *Phys. Rev. B* **40**, 11 370 (1989).
- ²⁰John M. Martinis and R. L. Kautz, *Phys. Rev. Lett.* **63**, 1507 (1989).
- ²¹Rosario Fazio and Gerd Schön, *Phys. Rev. B* **43**, 5307 (1991).
- ²²H. Grabert, P. Olschowski, U. Weiss, and P. Riseborough, *Phys. Rev. B* **36**, 1931 (1988).
- ²³H. S. J. van der Zant, H. A. Rijken, and J. E. Mooij, *J. Low Temp. Phys.* **82**, 67 (1991).
- ²⁴H. S. J. van der Zant, F. C. Fritschy, T. P. Orlando, and J. E. Mooij, *Phys. Rev. Lett.* **66**, 2531 (1991).